

# Triclosan Derivatives: Towards Potent Inhibitors of Drug-Sensitive and Drug-Resistant *Mycobacterium tuberculosis*

Joel S. Freundlich,<sup>[a, c]</sup> Feng Wang,<sup>[a]</sup> Catherine Vilchèze,<sup>[b]</sup> Gulcin Gulten,<sup>[a]</sup> Robert Langley,<sup>[a]</sup> Guy A. Schiehser,<sup>[c]</sup> David P. Jacobus,<sup>[c]</sup> William R. Jacobs, Jr.,<sup>[b]</sup> and James C. Sacchettini<sup>\*,[a]</sup>

*Triclosan has been previously shown to inhibit InhA, an essential enoyl acyl carrier protein reductase involved in mycolic acid biosynthesis, the inhibition of which leads to the lysis of Mycobacterium tuberculosis. Using a structure-based drug design approach, a series of 5-substituted triclosan derivatives was developed. Two groups of derivatives with alkyl and aryl substituents, respectively, were identified with dramatically enhanced potency against purified InhA. The most efficacious inhibitor displayed an IC<sub>50</sub> value of 21 nM, which was 50-fold more potent than triclosan. X-ray crystal structures of InhA in complex with four triclo-*

*san derivatives revealed the structural basis for the inhibitory activity. Six selected triclosan derivatives were tested against isoniazid-sensitive and resistant strains of M. tuberculosis. Among those, the best inhibitor had an MIC value of 4.7 µg mL<sup>-1</sup> (13 µM), which represents a tenfold improvement over the bacteriocidal activity of triclosan. A subset of these triclosan analogues was more potent than isoniazid against two isoniazid-resistant M. tuberculosis strains, demonstrating the significant potential for structure-based design in the development of next generation antitubercular drugs.*

## Introduction

For nearly fifty years, isoniazid (INH) has been utilized as a frontline drug to treat tuberculosis (TB).<sup>[1]</sup> INH is a key component of short course chemotherapy for TB treatment, which entails six months of daily administration, and is also the sole component for TB prophylaxis, which includes nine months of daily administration. The emergence of INH-resistant strains has compromised TB control programs worldwide.<sup>[2,3]</sup>

INH and ethionamide (ETH) are known to target the *Mycobacterium tuberculosis* enoyl acyl carrier protein (ACP) reductase (InhA),<sup>[4–7]</sup> validating it as an excellent antitubercular drug target. INH and ETH are prodrugs, and their activities are dependent on activation in *M. tuberculosis* by KatG, a catalase/peroxidase enzyme, and EthA, a flavin monooxygenase, respectively.<sup>[8,9]</sup> Upon activation, INH or ETH forms a covalent adduct with NAD cofactor, which inhibits InhA. As prodrugs, INH and ETH are highly specific and effective. However, mutations in activators *katG* and *ethA* have been linked to most of the clinical resistance in the diagnosed cases of drug-resistant TB.<sup>[9,10]</sup> Compounds that do not require activation and directly target InhA represent a promising approach to circumvent this resistance mechanism. The first report of such small-molecule InhA inhibitors came from our laboratories in 2003, featuring triclosan and two members of the Genzyme compound library.<sup>[11]</sup> Triclosan, for example, inhibits InhA without the need for prior activation, although its use as an antitubercular may be limited by its less than optimal bioavailability.<sup>[12]</sup> These small molecules, however, represent reasonable starting points for structure-based drug discovery efforts to afford effective InhA inhibitors. Aiding such an effort are several crystal structures, such as those of InhA:NADH,<sup>[13]</sup> InhA:NAD<sup>+</sup>:triclosan,<sup>[11]</sup> InhA:NAD<sup>+</sup>:Genz-10850,<sup>[11]</sup> InhA:NAD<sup>+</sup>:C16-substrate,<sup>[14]</sup> and InhA:INH-NAD<sup>+</sup><sup>[5]</sup> that were accessible at the outset of these investi-

gations. During the course of this work, Sullivan et al. reported the X-ray structures of two triclosan analogues with 5-alkyl (*n*-pentyl and *n*-octyl) moieties, lacking the two B-ring chlorines.<sup>[6]</sup> This collection of structures provided a precisely defined active site of InhA and a thorough understanding of the ligand–enzyme interactions that render potent enzyme inhibition.

One promising route for the design of potent InhA inhibitors involves triclosan, a commercially available compound that has been reported to inhibit the enoyl acyl ACP reductases (ENR) from several species, including *Plasmodium falciparum*,<sup>[15]</sup> *Escherichia coli*,<sup>[16]</sup> *Bacillus subtilis*,<sup>[17]</sup> *Brassica napus*,<sup>[18]</sup> and *Pseudomonas aeruginosa*.<sup>[19]</sup> The structures of ENR from *E. coli* (FabI),<sup>[20]</sup> *B. napus*,<sup>[18]</sup> *P. falciparum* (PfENR),<sup>[21]</sup> and *M. tuberculosis* (InhA)<sup>[11]</sup> bound with triclosan have been characterized. In our laboratories, a series of 5-substituted triclosan derivatives was designed and synthesized in order to optimize the potency of triclosan in parallel against both purified PfENR<sup>[23]</sup> and InhA. This report discusses these efforts focused specifically on the

[a] Dr. J. S. Freundlich, F. Wang,<sup>\*</sup> G. Gulten, R. Langley, Prof. Dr. J. C. Sacchettini  
Texas A&M University, Department of Biochemistry and Biophysics  
College Station, TX 77843-2128 (USA)  
Fax: (+1) 979-862-7638  
E-mail: sacchett@tamu.edu

[b] Dr. C. Vilchèze, Prof. Dr. W. R. Jacobs, Jr.  
Howard Hughes Medical Institute  
Department of Microbiology and Immunology  
Albert Einstein College of Medicine, Bronx, NY 10461 (USA)

[c] Dr. J. S. Freundlich, Dr. G. A. Schiehser, Dr. D. P. Jacobus  
Jacobus Pharmaceutical Company  
Princeton, NJ 08540 (USA)

[\*] Current address: The Scripps Research Institute Department of Chemistry and the Skaggs Institute for Chemical Biology

SAR developed versus purified InhA and INH-sensitive and resistant *M. tuberculosis*.

## Results and Discussion

Our efforts began with a survey of the complex structures of InhA bound with INH-NAD<sup>[5]</sup> and triclosan,<sup>[11]</sup> respectively. Two hydrophobic cavities capable of being filled were identified: the substrate-binding site and the pocket into which the isonicotinoyl group of INH-NAD protrudes. To date, all reported inhibitors of InhA occupied the hydrophobic cavity of the substrate-binding site, except the INH-NAD and ETH-NAD adducts. The isonicotinoyl moieties of the INH-NAD and ETH-NAD adducts were found in a hydrophobic pocket formed by movement of the side chain of Phe 149. The pocket was underneath the fatty acyl substrate-binding site (Figure 1) and, lined

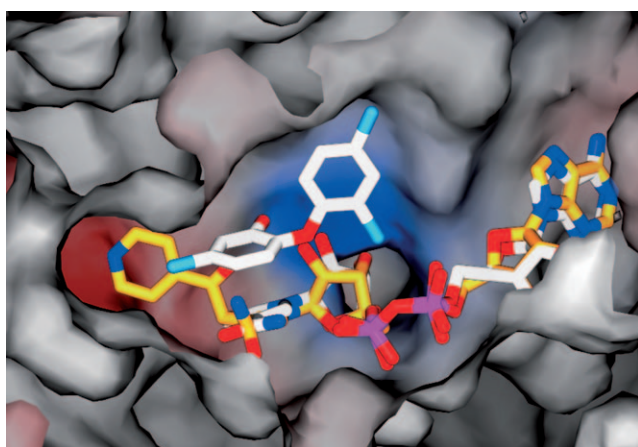


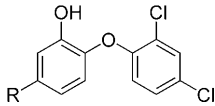
**Figure 1.** Cross-section through the surface of the InhA active site of superimposed structures of InhA in complex with the INH-NAD adduct and triclosan. The carbon atoms of the INH-NAD adduct and triclosan are colored in gold and white, respectively. Other atoms are colored according to the atom type: oxygen, red; nitrogen, blue; chlorine, cyan; phosphorus, purple. This figure was produced using Spock (version V1.ob170).<sup>[27]</sup>

predominantly by hydrophobic groups from the side chains of Tyr 158, Phe 149, Met 199, Trp 222, Leu 218, Met 155, Met 161, Gly 192, and Pro 193. This pocket may also serve as a portal to the external solvent to the left side of the active site (Figure 1). The active forms of both INH and ETH occupied the same pocket and were extremely potent against InhA ( $K_i = 5$  nM and 7 nM, respectively),<sup>[6,7]</sup> validating this cavity as a suitable site to target with new inhibitors. Superimposition of the structures of InhA:INH-NAD and InhA:NAD<sup>+</sup>:triclosan indicated that the chlorine atom at the 5-position of the triclosan A-ring was about 2 Å away from the binding pocket of isonicotinoyl moiety of the INH-NAD adduct and was in contact with Pro 193, Met 199, and Phe 149 through van der Waals interactions. Based on this structural information, we hypothesized that it may be possible to replace the 5-chloro with various moieties to occupy this isonicotinoyl binding pocket and, thus, increase the in vitro activity against InhA. It should be noted that this strategy contrasts with that of Sullivan et al. to extend relatively long *n*-alkyl chains off what is essentially the triclosan

5-position (in molecules where the two B-ring chlorines have been excised) to mimic substrate analogue *trans*-2-hexadecanoyl-(*N*-acetylcysteamine)thioester, whose structure with InhA we reported in 1999.<sup>[14]</sup>

A series of triclosan derivatives with modifications at the 5-position of triclosan was evaluated for their inhibition of purified InhA. These small molecules were prepared during the course of a concurrent program to investigate 5-substituted triclosan analogues as PfENR inhibitors.<sup>[23]</sup> Inhibitors with hydrophobic substituents, such as alkyl groups (compounds 2 and 7) were much more potent than those with hydrophilic substituents (compounds 3, 4 and 5) (Table 1). This result is

**Table 1.** In vitro activities of select triclosan derivatives against *M. tuberculosis* InhA.<sup>[a]</sup>

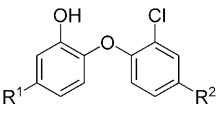
Compound		
	R	InhA IC <sub>50</sub> [nM]
triclosan	Cl	1100 ± 180
2	Me	800 ± 99
3	2 <i>H</i> -tetrazol-5-yl	> 10 000
4	COOH	> 10 000
5	C(O)NH <sub>2</sub>	> 10 000
6	Ph	> 10 000
7	CH <sub>2</sub> (C <sub>6</sub> H <sub>11</sub> )	110 ± 31

[a] Values reported as the mean ± standard error for at least three independent measurements.

consistent with our proposal that the 5-substituent of triclosan projects into a hydrophobic cavity of InhA. It is interesting to note the lack of activity of phenyl derivative 6, which may be explained by a potential steric clash with Phe 149 (as clarified below).

Following the initial modest activity of compounds 2 and 7, a series of 5-alkyl triclosan derivatives was examined for their inhibitory activity against InhA. Their potency against InhA appeared to increase with the chain length of the 5-alkyl groups (Table 2). Highest inhibitory potencies were observed for compounds 10 and 12 with four-carbon chains. Sullivan observed the same trend with 5-alkyl substituted, des-chloro triclosan derivatives.<sup>[22]</sup> It was found that the in vitro activity of those inhibitors was optimal at a carbon chain length of eight. Triclosan inhibitors show better in vitro activity than their des-chloro counterparts, with 5-substituents of the same carbon chain length, from the report by Sullivan et al. (ethyl, IC<sub>50</sub> = 120 ± 19 nM vs. 2000 ± 700 nM; *n*-butyl, IC<sub>50</sub> = 55 ± 20 nM vs. 80 ± 15 nM), suggesting that the two chlorine atoms on the B-ring contribute to the binding of the inhibitor to the enzyme. Molecular modeling suggests that this may be due to favorable van der Waals interactions of the 4'-Cl with Phe 97 and Met 103. These results imply that the hypothesis of Sullivan et al.<sup>[22]</sup> that the B-ring chlorines do not contribute to efficacy may not be correct.

**Table 2.** In vitro activities of select triclosan derivatives against *M. tuberculosis* InhA.<sup>[a]</sup>

Compound			InhA IC <sub>50</sub> [nM]
	R <sup>1</sup>	R <sup>2</sup>	
8	CH <sub>2</sub> CH <sub>3</sub>	Cl	120 ± 19
9	(CH <sub>2</sub> ) <sub>2</sub> CH <sub>3</sub>	Cl	91 ± 15
10	(CH <sub>2</sub> ) <sub>3</sub> CH <sub>3</sub>	Cl	55 ± 20
11	CH <sub>2</sub> CH(CH <sub>3</sub> ) <sub>2</sub>	Cl	96 ± 46
12	(CH <sub>2</sub> ) <sub>2</sub> CH(CH <sub>3</sub> ) <sub>2</sub>	Cl	63 ± 9
13	CH <sub>2</sub> CH(CH <sub>3</sub> )CH <sub>2</sub> CH <sub>3</sub>	Cl	130 ± 56
14	2-pyridyl	CN	> 10000
15	3-pyridyl	Cl	> 10000
16	4-pyridyl	CN	> 10000
17	CH <sub>2</sub> (2-pyridyl)	Cl	29 ± 11
18	CH <sub>2</sub> (3-pyridyl)	Cl	42 ± 10
19	CH <sub>2</sub> (4-pyridyl)	CN	75 ± 16
20	<i>o</i> -CH <sub>3</sub> -Ph	Cl	1300 ± 77
21	<i>o</i> -CH <sub>3</sub> -Ph	CN	> 10000
22	<i>m</i> -CH <sub>3</sub> -Ph	Cl	870 ± 110
23	<i>p</i> -F-Ph	Cl	> 10000
24	CH <sub>2</sub> Ph	Cl	51 ± 6
25	(CH <sub>2</sub> ) <sub>2</sub> Ph	Cl	21 ± 8
26	(CH <sub>2</sub> ) <sub>3</sub> Ph	Cl	50 ± 14

[a] Values reported as the mean ± standard error for at least three independent measurements.

The alkyl substituents investigated in previous studies were all linear in nature. In the present report, compounds **11**, **12**, and **13**, with  $\beta$ - or  $\gamma$ -branched methyl substituents, failed to improve upon the potency of their straight-chain counterparts of the same chain length (compounds **9** and **10**). Similarly, cyclohexylmethyl analogue **7** exhibited an IC<sub>50</sub> value of 110 nM. The 2.8 Å crystal structure of InhA in complex with compound **7** (Figure 2) was solved to provide a structural basis for the activity difference amongst the alkyl substituents. The crystal belonged to I4<sub>1</sub>22, a space group for InhA that has not been reported previously. It is worth noting that the substrate binding loop (residues 195–205) was ordered in the structure of InhA bound with compound **7**, while it has been disordered in the structures of InhA bound with triclosan, and all other triclosan derivatives solved to date. The structure was readily superimposed on that of InhA in complex with 5-pentyl-2-phenoxyphenol,<sup>[22]</sup> which intriguingly features a somewhat strained C4–C5 portion of the pendant alkyl chain, and the C16 substrate analogue<sup>[14]</sup> (overlapping the position of C4 to C7 of the U-shaped acyl chain). The 5-cyclohexylmethyl group formed predominantly hydrophobic interactions with the side chains of Phe149, Ile215, Leu218, Met155, Tyr158, and Met199. Based on this structure, we hypothesized that 5-substituents with a longer alkyl chain would create more extensive hydrophobic interactions in this pocket. Therefore, it was not surprising that the potency of the 5-alkyl triclosan analogues increased with the chain length. However, it is not so obvious from a structural point of view why our limited subset of methyl-branched inhibitors do not exhibit greater potency than the nonbranched inhibitors of the same chain length. A

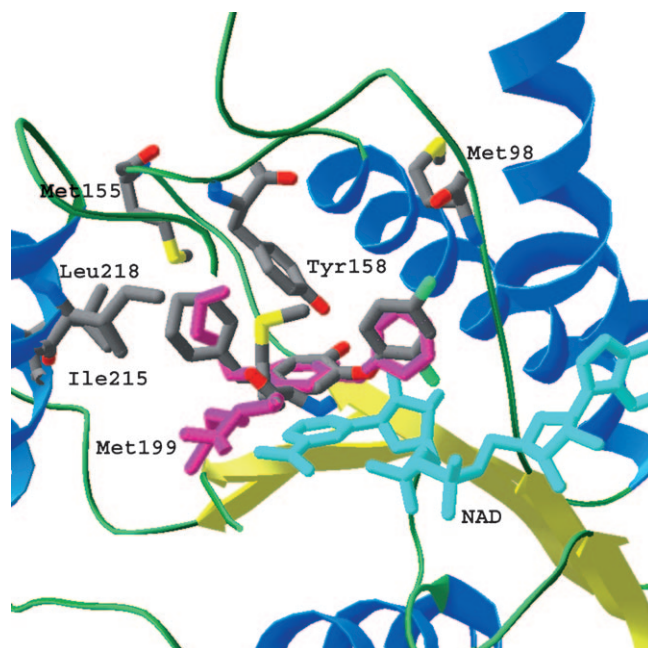


**Figure 2.** The superposition of crystal structures of InhA (ribbons and tubes, key residues in stick format) in complex with 5-pentyl-2-phenoxyphenol<sup>[22]</sup> (purple) and compound **7** (carbon atoms in gray) in the presence of NAD<sup>+</sup> (cyan). The B-ring of the 5-pentyl triclosan analogue was in a different orientation from **7**, because of the lack of two chlorides. The cyclohexylmethyl group of compound **7** was in a similar position to the pentyl group of 5-pentyl triclosan analogue. This figure, in addition to Figure 3 and 4, was made using SwissPDB viewer (version 3.7).<sup>[28]</sup>

possible explanation could be steric clashes with one or more of the side chains of Phe149, Tyr158, and Met199 with the branched methyl groups. Compared to the structure of InhA bound with the 5-pentylphenol derivative designed by Sullivan et al., the side chain of Met199 on the substrate-binding loop flipped ~100° to form a hydrophobic interaction with the cyclohexyl group at a distance of 3.6 Å. In addition, the B-ring of compound **7** also rotated ~30° from its position in 5-pentyl-2-phenoxyphenol to allow the 4'-chloride to form a weak hydrogen-bonding interaction with the amide NH of Met98 at a distance of 3.2 Å.

Analogues of phenyl **6** were examined to improve upon the surprisingly poor enzyme inhibition observed (Table 2). Pyridyl derivatives **14**–**16** and simple phenyl analogues **20**–**23** were also poor InhA inhibitors. Although the crystal structures for InhA bound with 5-phenyl or 5-pyridyl triclosan analogues have not been obtained to date, the inhibitors were modeled<sup>[24]</sup> into the active site based on the structure of InhA:triclosan. A directly attached aryl group at the 5-position appeared to be too close to the side chain of Phe149 (shortest distance was ~1.4 Å between the aryl substituent and the phenyl group of Phe149), leading to steric clashes. The hydrophobic pocket of interest was separated from the 5-position by a distance of 2.5 Å.

Therefore, to reorient and better position the hydrophobic aryl group into the target pocket, a linker varying from 1–3 carbons was incorporated between the aryl substituent and the 5-position carbon on the A-ring (Table 2). Consistent with the



molecular modeling results, an evaluation of 5-position substituents of the type  $(\text{CH}_2)_n\text{Ar}$  demonstrated that carbon linkers significantly increased the inhibitory potency versus purified enzyme. Among them, compound **25** had the highest potency ( $\text{IC}_{50} = 21 \text{ nM}$ ), representing a 50-fold increase compared to triclosan. It is the most potent triclosan derivative against purified InhA we have studied to date. Compounds **24** and **26**, with similar activities against InhA (**24**,  $\text{IC}_{50} = 51 \text{ nM}$ ; **26**,  $50 \text{ nM}$ ), were also active inhibitors. The crystal structures of InhA bound with **24** and **25** showed that the  $(\text{CH}_2)_n\text{Ar}$  group extended into the pocket and formed hydrophobic interactions with residues Leu218, Ile215, Phe149, Met199, and Pro193 (Figure 3). The triclosan backbone atoms of com-

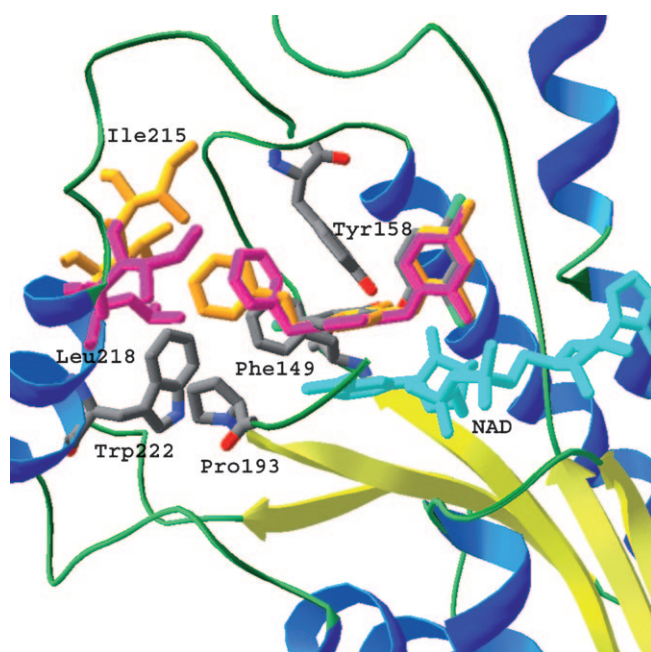


**Figure 3.** The superposition of crystal structures of InhA (ribbons and tubes, key residues in stick format) in complex with triclosan (carbon atoms in gray), compound **24** (purple), and compound **25** (gold) in the presence of  $\text{NAD}^+$  (cyan). The 5-phenyl groups of compounds **24** and **25** are shown making van der Waals contacts with the side chains of Tyr158, Pro193, Leu218, Ile215, and Phe149. The movements of Ile215 and Leu218 in response to the triclosan 5-substituent are depicted by showing this residue in stick format with the coloring of the respective ligand. It should be noted that Met199 is not depicted for the sake of clarity.

pounds **24** and **25** were in nearly identical positions, but their 5-substituents were clearly different. The phenyl group of derivative **24** was positioned in the center of the binding pocket, while the phenyl group of derivative **25** protruded  $\sim 2 \text{ \AA}$  deeper into, and was closer to the end of, the binding pocket due to the longer carbon linker. Thus, compound **25** additionally engaged Trp222 in a hydrophobic interaction. The side chains of Leu218 and Ile215 rotated  $30^\circ$  and shifted  $1.5 \text{ \AA}$ , respectively, to accommodate the phenyl ring of compound **25**, which also flipped  $\sim 70^\circ$  from the position of the phenyl group of compound **24**. All of these conformational changes suggest that there were more hydrophobic interactions between the active site residues and the 5-substituent of compound **25**

than that of compound **24**, which may explain why compound **25** was twice as potent than compound **24** against InhA.

To further increase the potency of the  $5-(\text{CH}_2)_n\text{Ar}$  series through potential mimicry of the INH-NAD isonicotinoyl moiety, derivatives with  $5-\text{CH}_2(n\text{-pyridyl})$  ( $n=2, 3$ , and  $4$ ) substituents (compounds **17–19**) were examined for in vitro activity. In the crystal structure of InhA:INH-NAD,<sup>[5]</sup> the pyridyl group of the INH-NAD adduct formed a hydrogen-bonding interaction with a buried water molecule. Without a carbon linker, the 5-pyridyl triclosan derivatives **14–16** showed very low activity against InhA ( $\text{IC}_{50} > 10 \text{ }\mu\text{M}$ ), presumably due to a steric clash with Phe149. In contrast, with a one-carbon linker, pyridyl analogues **17–19** were all potent inhibitors ( $\text{IC}_{50} < 80 \text{ nM}$ ), and their  $\text{IC}_{50}$  values were in the order **17** < **18** < **19**. Compared to benzyl derivative **24**, the activity of **17** increased approximately twofold while the activity of compound **18** increased only slightly, and compound **19** was slightly less potent. The structure of InhA: $\text{NAD}^+:\textbf{17}$  demonstrated that the pyridyl ring of derivative **17** extended into the substrate-binding site to form hydrophobic interactions with the side chains of Tyr158 and Phe149 (Figure 4). These interactions are similar to those of the phenyl group in InhA: $\text{NAD}^+:\textbf{24}$ . However, the nitrogen atom on the 2-position of the pyridyl ring also formed a hydrogen-bonding interaction with the side chain carboxylate of Glu219 through a water molecule. Modeling studies indicated that similar interactions could also exist for **18**, but were not likely for **19**, based on the distance between the pyridyl nitrogen atom and the side chain oxygen of

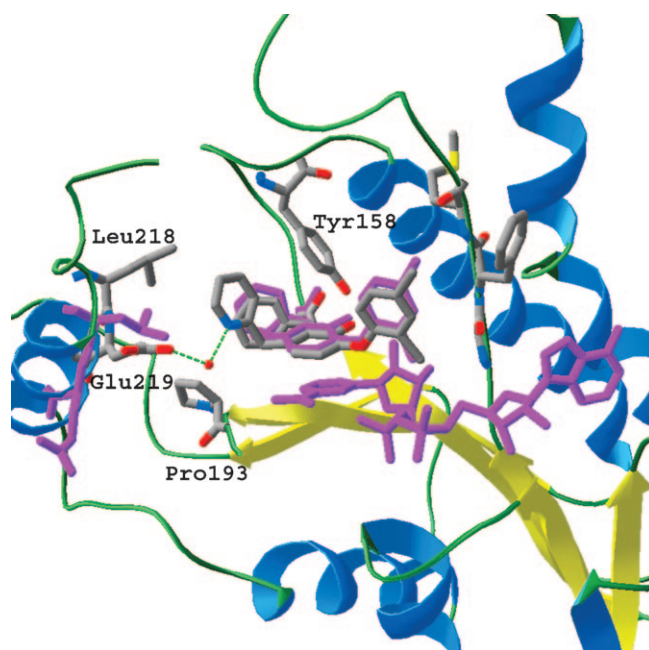


**Figure 4.** The superposition of crystal structures of InhA (ribbons and tubes, key residues in stick format) in complex with triclosan (purple) and compound **17** (carbon atoms in gray) in the presence of  $\text{NAD}^+$  (cyan). The nitrogen atom on the pyridyl ring formed a hydrogen-bonding interaction with the side chain of Glu219 through a water molecule. The side chain of Glu219 rotated  $90^\circ$  from its original position (purple) to form this hydrogen-bonding interaction. It should be noted that Phe149 is not depicted for the sake of clarity.

Glu219. The nitrogen atom of **19** potentially pointed to the hydrophobic side chains of residues Met155 and Leu218, which may not be favored energetically. The superimposition of InhA:NAD<sup>+</sup>:**17** and InhA:NAD<sup>+</sup>:triclosan,<sup>[11]</sup> demonstrated movement of both Glu219 and Leu218 to accommodate the 5-pyridylmethyl moiety.

A comparison of the X-ray crystal structures of bound compounds **7**, **17**, **24**, and **25** with that of INH–NAD (PDB code 1ZID) is instructive. At the outset, our goal was to reach from the 5-position of triclosan into the isonicotinoyl-binding pocket. The Phe149 side chains from the four triclosan analogue structures overlapped well with each other, but not that of 1ZID. In 1ZID, the isonicotinoyl group of INH was stabilized by the rotation of Phe149. The various triclosan 5-substituents, however, did not occupy the same volume as the isonicotinoyl group, orienting similarly to the C16 chain of the structurally characterized substrate analogue<sup>[14]</sup> and the appended alkyl substituent in the structures reported by Sullivan et al.,<sup>[22]</sup> and thus did not perturb Phe149. In the 1ZID structure, the movement of Phe149 evidently displaced Tyr158. While this motion was tolerated in 1ZID, in the triclosan structures, the phenol moiety is positioned through an interaction with the hydroxyl of Tyr158. Loss of the triclosan phenol–Tyr158 interaction would most likely result in complete loss of inhibitor binding, supported by the observed weak inhibitory activity of desphenol triclosan analogues against InhA. Thus, while the triclosan analogues can attempt to place substituents proximal to the INH binding pocket, they cannot occupy the exact volume of the isonicotinoyl moiety, as this would ultimately require the movement of Phe149 and Tyr158, thus losing a key hydrogen-bonding interaction with Tyr158.

The activities of three 5-alkyl (**7**, **10**, and **11**) and three 5-aryl triclosan derivatives (**24**, **25**, and **26**) against six different *M. tuberculosis* strains were assayed (Table 3). Among these strains, H37Rv is the *M. tuberculosis* wild-type, sensitive to isoniazid. The InhA(S94 A) strain, carrying the *inhA*(S94A) allele, has been demonstrated to confer resistance to isoniazid through the weakening of co-factor binding.<sup>[6]</sup> The InhA(C-15T) strain is a *M. tuberculosis* spontaneous mutant carrying the *inhA* expression region mutation (C-15T).<sup>[6]</sup> It has been shown that the C-15T *inhA* promoter mutation mediates enhanced transcription of *inhA*, resulting in INH and ETH resistance. The  $\Delta katG$  mutant features the complete deletion of the *katG* gene and, thus, INH activation cannot take place. Most significantly, strains 12081

and 5071 are multidrug resistant clinical isolates from Mexico that are INH resistant without known mutations in *katG*, *inhA*, *ndh*, and *ahpC*. The 12081 (SCG V) strain was, in our hands, resistant to INH, streptomycin, and rifampicin, while 5071 (SCG 3b) was resistant to only INH and streptomycin.

The selected six compounds with high potency against InhA in vitro ( $IC_{50} \leq 110$  nM) all demonstrated good antitubercular activity against the wild-type H37Rv strain, exhibiting improvements over the whole-cell efficacy of triclosan. Clearly, the 5-chloro group of triclosan is not optimal and the use of larger and more hydrophobic moieties is advantageous both in terms of InhA inhibition and whole-cell potency. The most active compound, **26** (MIC = 13  $\mu$ M), was superior to that of ETH (MIC = 18  $\mu$ M),<sup>[6]</sup> while being greater than tenfold more potent than triclosan. The activities of these compounds against purified InhA and cultured tuberculosis strains generally correlated well. For example, compound **10**, which had two-fold higher activity against InhA than compound **11**, also exhibited twofold better antitubercular activity. This supports a hypothesis that the straight chain 5-alkyl substituent has an advantage over the analogous branched derivative. In addition, compound **26**, which displayed the highest antitubercular activity in the series, also had the second highest potency against InhA. Exceptions may be noted such as with compound **25**, which showed the highest potency among the (CH<sub>2</sub>)<sub>n</sub>Ar series and yet the worst antitubercular activity. As may be expected, a number of factors other than in vitro efficacy against purified InhA, including pharmacokinetic parameters, contribute to the whole-cell inhibition of mycobacterial growth.

It is interesting to compare the H37Rv data for 5-*n*-butyltriclosan (**10**) and the corresponding des-chloro analogue of Sullivan and co-workers. While compound **10** ( $IC_{50}$  = 55 nM) was slightly more active than its des-chloro analogue against InhA ( $IC_{50}$  = 80 nM),<sup>[22]</sup> the des-chloro compound (MIC = 10.8  $\mu$ M) was more efficacious against H37Rv compared with compound **10** (MIC = 30  $\mu$ M). It should be noted that the most potent triclosan analogue reported to date is the *n*-octyl analogue reported by Sullivan et al. (InhA,  $IC_{50}$  = 5.0 nM; H37Rv, MIC = 6.5  $\mu$ M).<sup>[22]</sup>

Triclosan has previously been reported to display promising activity against both INH sensitive and resistant *M. tuberculosis* strains.<sup>[11,22]</sup> We next examined five strains against which the triclosan family of compounds had not been tested. Compared to their efficacy against the wild-type strain, five of the six ana-

**Table 3.** Minimum Inhibitory Concentration (MIC) values of triclosan derivatives against wild-type and mutant *M. tuberculosis* strains.

Compound	H37Rv [ $\mu$ g mL <sup>-1</sup> ] ([ $\mu$ M])	H37Rv <i>inhA</i> (S94 A) [ $\mu$ g mL <sup>-1</sup> ] ([ $\mu$ M])	H37Rv PmabAinhA (C-15T) [ $\mu$ g mL <sup>-1</sup> ] ([ $\mu$ M])	H37Rv $\Delta katG$ [ $\mu$ g mL <sup>-1</sup> ] ([ $\mu$ M])	Clinical isolate 12081 [ $\mu$ g mL <sup>-1</sup> ] ([ $\mu$ M])	Clinical isolate 5071 [ $\mu$ g mL <sup>-1</sup> ] ([ $\mu$ M])
<b>7</b>	9.4 (27)	37 (110)	37 (110)	19 (55)	37 (110)	4.7 (13)
<b>10</b>	9.4 (30)	37 (120)	37 (120)	19 (60)	37 (120)	4.7 (15)
<b>11</b>	19 (60)	37 (120)	37 (120)	37 (120)	75 (240)	19 (60)
<b>24</b>	9.4 (27)	75 (220)	37 (110)	19 (55)	75 (220)	9.4 (27)
<b>25</b>	19 (52)	75 (210)	75 (210)	37 (110)	75 (210)	19 (52)
<b>26</b>	4.7 (13)	19 (50)	19 (50)	9.4 (26)	37 (100)	4.7 (13)
INH	0.060 (0.44)	0.50 (3.6)	0.80 (5.8)	> 200 (> 1400)	1.0 (7.3)	8.0 (56)
triclosan	40 (140)					

logues examined showed 4–8-fold lower activity against the InhA(S94A) and InhA(C-15T) strains. This was slightly lower, yet still comparable in magnitude, to the 8- and 13-fold losses in potency for INH against these two strains, respectively. The InhA(C-15T) strain has a higher expression of InhA, which leads to resistance to compounds that target the protein. The resistance to triclosan by InhA(S94A) strains of either *M. tuberculosis* or other bacteria has not been previously reported to the best of our knowledge. Mutation of the G93V in FabI, a residue conserved in InhA, has previously been found to confer *E. coli* resistance to triclosan.<sup>[25]</sup> The *inhA*(S94A) mutation has been demonstrated to decrease the efficacy of INH by weakening the binding of INH–NAD.<sup>[6]</sup> Comparatively, the binding of triclosan and its analogues to InhA depends greatly on the interaction between the diaryl ether scaffold and NAD<sup>+</sup>. Quemard and co-workers reported that the S94A mutation weakened the binding of NADH by ~500-fold.<sup>[26]</sup> It is proposed that the same mutation may decrease the stability of the InhA: NAD<sup>+</sup>:triclosan derivative complex and, thereby, diminish inhibition. The resistance of the InhA(S94A) and InhA(C-15T) strains to triclosan derivatives is supportive of our proposal that the target of these triclosan relatives is indeed InhA.

The activity of the triclosan analogue subset against the  $\Delta katG$  mutant further substantiates the potential advantage of these InhA inhibitors over INH. While INH was more than 3000-times less active against the  $\Delta katG$  mutant, the triclosan analogues were only twofold less active, as measured by their MIC values. This is consistent with our genetic, enzymatic, and X-ray crystallographic data that demonstrate InhA inhibition by the triclosan family without the need for activation. It, therefore, follows that one would expect a lack of cross-resistance with many INH-resistant *M. tuberculosis* strains, where the *katG* mutations represent the dominant allele conferring resistance. Sullivan and colleagues have also demonstrated their phenol diaryl ethers to not suffer significant losses in potency against clinical isolates with varying degrees of INH resistance.<sup>[22]</sup>

The two clinical strains shown in Table 3 were much more sensitive to the triclosan analogues compared with INH. Strain 12081 afforded 17-fold resistance to INH, which was reduced to a 4–8 factor resistance against the triclosan subset. Against clinical isolate 5071, the triclosan subset maintained or improved (in two cases by twofold) their respective wild-type potencies. These results should be contrasted to the *greater than two orders of magnitude* resistance conferred against INH. Thus, triclosan analogues may, in general, offer a high degree of activity against INH resistant *M. tuberculosis*.

## Conclusions

The efficacy of these 5-substituted triclosan analogues has been shown to be tunable through a structure-based optimization of the 5-position. Novel analogues afforded a 50-fold increase in InhA inhibition and tenfold in bacteriocidal activity. Most significantly, these triclosan derivatives demonstrated efficacy against INH-resistant laboratory and clinical strains of *M. tuberculosis*. Further studies of triclosan and other small-molecule inhibitors of InhA hold significant promise for the de-

livery of novel antitubercular agents that are effective against drug-resistant *M. tuberculosis*. Current efforts are underway to examine the physicochemical properties of our most promising analogues. Substitution of the phenol will be investigated to avoid potential liabilities due to rapid Phase II metabolism,<sup>[12]</sup> preceding clearance. In addition, other modifications to the A- and/or B-rings of the diaryl ether scaffold can be envisioned that would potentially increase the stability of these derivatives to oxidative metabolism, while not sacrificing efficacy.

## Experimental Section

**Triclosan analogue synthesis:** The small molecules tested against InhA and the mycobacterial strains were synthesized as described previously in the literature.<sup>[23]</sup>

**Cloning, expression, and purification for *Mycobacterium tuberculosis inhA*:** *M. tuberculosis inhA* was cloned into *E. coli* BL21 (DE3) as described previously.<sup>[13]</sup> The transformed *E. coli* were cultured in Terrific Broth media with 50  $\mu\text{g mL}^{-1}$  carbenicillin at 37 °C until an OD<sub>600</sub> of 0.8 was observed. *inhA* expression was induced for 20 h at 16 °C through addition of 1 mM isopropyl  $\beta$ -D-thiogalactopyranoside. The resulting cells harvested through centrifugation were resuspended in 50 mM PIPES (pH 6.8) and 1 mM phenylmethylsulfonyl fluoride and lysed via French press. Exposure to DNase I was followed by removal of insoluble material through centrifugation. The supernatant was subjected to a HiTrap Blue Sepharose column (AP Biotech), pre-equilibrated with the same buffer, using a fast protein liquid chromatography system and eluted through a NaCl gradient (0–2 M). Elution with 0.9 M NaCl solution afforded fractions containing InhA that were subsequently subjected to an octyl-sepharose column (AP Biotech), pre-equilibrated with 1 M NaCl, and eluted through a NaCl gradient (1–0 M). Pooling of InhA fractions and gel filtration through a Superdex 200 column were carried out to separate monomeric protein from aggregated material. SDS-PAGE and Coomassie Blue staining were consistent with homogeneous InhA, yielding 40 mg L<sup>-1</sup> from *E. coli* culture.

**InhA enzyme assay:** Experiments were carried out utilizing a Cary100 Bio spectrophotometer at 25 °C, through monitoring the oxidation of NADH to NAD<sup>+</sup> at 340 nm. Reactions were initiated via addition of dodecenoyl-CoA (50  $\mu\text{M}$ ) substrate to mixtures containing InhA (5 nM), NADH (100  $\mu\text{M}$ ), and inhibitor (1–10 000 nM). The IC<sub>50</sub> values were determined from a dose-response plot of enzyme fractional activity versus the concentration of inhibitor.

**Antimycobacterial assays:** The relevant *M. tuberculosis* strains were obtained from laboratory stocks and grown in Middlebrook 7H9 medium (Difco), supplemented with 10% (v/v) OADC enrichment (Difco), 0.2% (v/v) glycerol, and 0.05% (v/v) tyloxapol to an OD<sub>600</sub> of ~1.0. The cultures were diluted 4 logs and 0.1 mL of the resulting dilutions were inoculated into 2 mL of Middlebrook 7H9 media with varying concentrations of inhibitor. The cultures were incubated with shaking at 37 °C for four weeks. The MIC was defined as the concentration of inhibitor that prevented visible mycobacterial growth.

**Crystallization of InhA with selected inhibitors:** The hanging drop vapor diffusion method was utilized. Typically, InhA was incubated with an inhibitor and NAD<sup>+</sup> in the molar ratio of 1:2:100 for 2 h. Co-crystallization was then attempted in hanging droplets con-



**Table 4.** Data collection and refinement statistics for reported X-ray structures.<sup>[a]</sup>

	InhA:7	InhA:17	InhA:24	InhA:25
Maximum resolution [Å]	1.97	1.98	2.30	2.80
Space group	I4(1)22	C2	C2	I4(1)22
a [Å]	90.0	125.6	125.6	90.0
b [Å]	90.0	92.3	92.4	90.0
c [Å]	183.9	103.0	102.4	183.1
$\alpha$ [°]	90.0	90.0	90.0	90.0
$\beta$ [°]	90.0	106.4	106.5	90.0
$\gamma$ [°]	90.0	90.0	90.0	90.0
Unique reflections <sup>[b]</sup>	27 204 (2964)	71 784 (6260)	43 113 (3799)	9708 (1063)
$R_{\text{sym}}$ [%]	6.0 (74.3)	9.9 (70.5)	10.3 (88.3)	12.8 (82.3)
Completeness [%]	99.8 (100)	87.3 (65.5)	99.1 (98.5)	99.8 (100)
Redundancy	10.2 (10.0)	3.7 (2.1)	5.3 (4.9)	8.5 (8.6)
$I/\sigma$	42.5 (4.3)	15.7 (1.3)	28.6 (3.3)	22.3 (3.7)
Resolution range [Å]	19.92–1.97	19.96–1.98	19.85–2.30	19.85–2.8
# reflections	25 755	68 885	46 976	9157
# atoms per subunit				
Protein	1994	7826	7739	1994
Cofactor (NAD)	52	176	176	52
Ligand	22	88	88	23
Solvent	168	703	253	11
$R_{\text{cryst}}$ [%]	20.7	20.0	20	22.1
$R_{\text{free}}$ [%]	25.2	25.3	26	26.8
Average B-factors [Å <sup>2</sup> ]	35.0	1.98	40.2	54.8

[a] PDB accession code are 3FNG (7), 3FNE (17), 3FNF (24), and 3FNH (25). [b] The value of the highest resolution shell is given in parentheses.

sisting of 2  $\mu\text{L}$  of 10  $\text{mg mL}^{-1}$  protein solution and 2  $\mu\text{L}$  of buffer (20% PEG 3350, 6% DMSO, 0.1 M *N*-(2-acetamido)iminodiacetic acid pH 6.8, 0.08 M  $\text{NH}_4\text{OAc}$ ) at 16 °C in Linbro plates against 0.5 mL of the same buffer. Protein crystals were observed after approximately four days.

**Data collection and processing:** Data were collected at 121 K utilizing cryo-protection solution with reservoir solution and an added 30% ethylene glycol. A crystal of InhA:17 diffracted X-rays to 1.98 Å at beam line 23ID at the Advanced Photo Source (APS), Argonne National Laboratory. Crystals of InhA:24, InhA:25 and InhA:7 diffracted X-rays to 2.30 Å, 2.80 Å and 1.98 Å, respectively, using a Rigaku Raxis detector coupled to an X-ray generator with a copper rotating anode ( $\text{Cu}_{\text{K}\alpha}$ ,  $\lambda = 1.54$  Å). Diffraction data was obtained from a single crystal with 0.5° degree oscillation widths for a range of 180°. The data were integrated and reduced using HKL2000 (Table 4).<sup>[29]</sup>

**Structure determination and model refinement:** Initial phases of the InhA:inhibitor complexes were obtained through molecular replacement utilizing the apo-InhA structure (PDB code: 1ENY) and refined with CCP4<sup>[30]</sup> (Table 4). Electron density maps were calculated and additional density was found, consistent with the respective inhibitor. The inhibitor was fit into the additional density and the whole model was rebuilt utilizing XtalView.<sup>[24]</sup> In the final refinement cycles, water molecules were added into peaks above 3- $\sigma$  of the  $F_o - F_c$  electron density maps, such that the water molecules were within hydrogen-bonding distance from the appropriate protein atoms. Final statistics are in Table 4.

## Acknowledgements

We would like to thank John Kim (AECOM) and Dr. Tsungda Hsu (AECOM) for preparing the *M. tuberculosis*  $\Delta\text{katG}$  strain and Professor David Alland (UMDNJ) for donation of the 5071 and 12081 clinical isolates. This work has been supported by funding from the Medicines for Malaria Venture, the National Institutes of Health (PO1A1068135), and the Robert A. Welch Foundation (A-0015).

**Keywords:** antibiotics • drug resistance • fatty acids • triclosan • tuberculosis

- [1] C. Vilchèze, W. R. Jacobs Jr., *Annu. Rev. Microbiol.* **2007**, *61*, 35–50.
- [2] CDC, *MMWR Morb. Mortal. Wkly. Rep.* **2006**, *55*, 301–305; <http://www.cdc.gov/mmwr/PDF/wk/mm5511.pdf>.
- [3] J. Crofton, P. Chaulet, D. Maher, J. Grosset, W. Harris, H. Norman, M. Iseman, B. Watt, *Guidelines for the management of Multidrug-resistant Tuberculosis*, World Health Organization, Geneva, **1997**.
- [4] A. Banerjee, E. Dubnau, A. Quemard, V. Balasubramanian, K. S. Um, T. Wilson, D. Collins, G. de Lisle, W. R. Jacobs, Jr., *Science* **1994**, *263*, 227–230.
- [5] D. A. Rozwarski, G. A. Grant, D. H. Barton, W. R. Jacobs, Jr., J. C. Sacchettini, *Science* **1998**, *279*, 98–102.
- [6] C. Vilchèze, F. Wang, M. Arai, M. H. Hazbón, R. Colangeli, L. Kremer, T. R. Weisbrod, D. Alland, J. C. Sacchettini, W. R. Jacobs, Jr., *Nat. Med.* **2006**, *12*, 1027–1029.
- [7] F. Wang, R. Langley, G. Gulten, L. G. Dover, G. S. Besra, W. R. Jacobs, Jr., J. C. Sacchettini, *J. Exp. Med.* **2007**, *204*, 73–78.
- [8] A. E. DeBarber, K. Mdluli, M. Bosman, L. G. Bekker, C. E. Barry 3rd, *Proc. Natl. Acad. Sci. USA* **2000**, *97*, 9677–9682.
- [9] G. P. Morlock, B. Metchock, D. Sikes, J. T. Crawford, R. C. Cooksey, *Antimicrob. Agents Chemother.* **2003**, *47*, 3799–3805.
- [10] M. H. Hazbón, M. Brimacombe, M. Bobadilla del Valle, M. Cavatore, M. I. Guerrero, M. Varma-Basil, H. Billman-Jacobe, C. Lavender, J. Fyfe, L. García-García, C. I. León, M. Bose, F. Chaves, M. Murray, K. D. Eisenach, J. Sifuentes-Osornio, M. D. Cave, A. Ponce de León, D. Alland, *Antimicrob. Agents Chemother.* **2006**, *50*, 2640–2649.
- [11] M. R. Kuo, H. R. Morbidoni, D. Alland, S. F. Sneddon, B. B. Gourlie, M. M. Staveski, M. Leonard, J. S. Gregory, A. D. Janjigian, C. Yee, J. M. Musser, B. Kreiswirth, H. Iwamoto, R. Perozzo, W. R. Jacobs, Jr., J. C. Sacchettini, D. A. Fidock, *J. Biol. Chem.* **2003**, *278*, 20851–20859.
- [12] L.-Q. Wang, C. N. Falany, M. O. James, *Drug Metab. Dispos.* **2004**, *32*, 1162–1169.
- [13] A. Dessen, A. Quemard, J. S. Blanchard, W. R. Jacobs, Jr., J. C. Sacchettini, *Science* **1995**, *267*, 1638–1641.
- [14] D. A. Rozwarski, C. Vilchèze, M. Sugantino, R. Bittman, J. C. Sacchettini, *J. Biol. Chem.* **1999**, *274*, 15582–15589.
- [15] N. Surolia, A. Surolia, *Nat. Med.* **2001**, *7*, 167–173.
- [16] R. J. Heath, Y.-T. Yu, M. A. Shapiro, E. Olson, C. O. Rock, *J. Biol. Chem.* **1998**, *273*, 30316–30320.
- [17] R. J. Heath, N. Su, C. K. Murphy, C. O. Rock, *J. Biol. Chem.* **2000**, *275*, 40128–40133.

- [18] A. Roujeinikova, C. W. Levy, S. Rowsell, S. Sedelnikova, P. J. Baker, C. A. Minshull, A. Mistry, J. G. Colls, R. Camble, A. R. Stuitje, A. R. Slabas, J. B. Rafferty, R. A. Pauptit, R. Viner, D. W. Rice, *J. Mol. Biol.* **1999**, *294*, 527–535.
- [19] T. T. Hoang, H. P. Schweizer, *J. Bacteriol.* **1999**, *181*, 5489–5497.
- [20] C. W. Levy, A. Roujeinikova, S. E. Sedelnikova, P. J. Baker, A. R. Stuitje, A. R. Slabas, D. W. Rice, J. B. Rafferty, *Nature* **1999**, *398*, 383–384.
- [21] R. Perozzo, M. Kuo, A. S. Sidhu, J. T. Valiyaveetil, R. Bittman, W. R. Jacobs, Jr., D. A. Fidock, J. C. Sacchettini, *J. Biol. Chem.* **2002**, *277*, 13106–13114.
- [22] T. J. Sullivan, J. J. Truglio, M. E. Boyne, P. Novichenok, X. Zhang, C. F. Stratton, H. J. Li, T. Kaur, A. Amin, F. Johnson, R. A. Slayden, C. Kisker, P. J. Tonge, *ACS Chem. Biol.* **2006**, *1*, 43–53.
- [23] J. S. Freundlich, F. Wang, H.-C. Tsai, M. Kuo, H.-M. Shieh, J. W. Anderson, L. J. Nkrumah, J.-C. Valderramos, M. Yu, T. R. S. Kumar, S. G. Valderramos, W. R. Jacobs Jr., G. A. Schiehser, D. P. Jacobus, D. A. Fidock, J. C. Sacchettini, *J. Biol. Chem.* **2007**, *282*, 25436–25444.
- [24] D. E. McRee, *J. Struct. Biol.* **1999**, *125*, 156–165.
- [25] L. M. McMurtry, M. Oethinger, S. B. Levy, *Nature* **1998**, *394*, 531–532.
- [26] A. Quemard, J. C. Sacchettini, A. Dessen, C. Vilchèze, R. Bittman, W. R. Jacobs, Jr., J. S. Blanchard, *Biochemistry* **1995**, *34*, 8235–8241.
- [27] J. A. Christopher, SPOCK: The Structural Properties Observation and Calculation Kit. Program Manual., The Center for Macromolecular Design, Texas A&M University, College Station, TX., **1998**.
- [28] N. Guex, M. C. Peitsch, *Electrophoresis* **1997**, *18*, 2714–2723.
- [29] Z. Otwinowski, W. Minor, *Methods Enzymol.* **1997**, *276*, 307–326.
- [30] Collaborative Computational Project, Number 4, *Acta Crystallogr. D Biol. Crystallogr.* **1994**, *50*, 760–763.

---

Received: August 1, 2008

Revised: October 24, 2008

Published online on January 7, 2009